Adiabatic energy levels and electric dipole moments of Rydberg states of Rb_2 and Cs_2 dimers

A. A. Khuskivadze,[1] M. I. Chibisov,[2] and I. I. Fabrikant[1]
[1]*Department of Physics and Astronomy, University of Nebraska, Lincoln, Nebraska 68588-0111*
[2]*Russian Research Center "Kurchatov Institute," Institute of Nuclear Fusion, Moscow 123182, Russia*
(Received 13 May 2002; published 15 October 2002)

We calculate potential energy curves for heavy alkali-metal dimers, Rb_2 and Cs_2 in which one of the atoms is in a highly excited Rydberg states. The method combines numerical integration of coupled equations, describing interaction of electron with the ground-state atom in the field of the Coulomb core of the Rydberg atom, with subsequent matching of the obtained wave function with the Coulomb Green's function in the form of the Kirchhoff integral. The spin-orbit interaction for the Rydberg electron is also included. The results show the existence of several groups of states. Most interesting of them are dominated either by the ^3S symmetry near the ground-state atom or by the ^3P_J symmetry, $J=0,1,2$. All states, except the $^3P_1$ state, exhibit oscillatory dependence of energy on the internuclear distance that can support long-range molecular Rydberg states [e.g., "trilobite states" for the ^3S symmetry, Greene *et al.*, Phys. Rev. Lett. **85**, 2458 (2000)]. These states possess large diagonal and transition dipole moments which are expressed analytically in terms of the Coulomb wave functions and calculated in a broad range of internuclear separations.

DOI: 10.1103/PhysRevA.66.042709 PACS number(s): 34.10.+x, 34.70.+e

I. INTRODUCTION

Molecular Rydberg states play an important role in a variety of collision processes such as inelastic collisions of Rydberg atoms with ground-state atoms, particularly collisional broadening of Rydberg states [1–3], charge transfer in ion-atom and atom-atom collisions [4], dissociative recombination [5]. Recently the interest to molecular Rydberg states has increased due to theoretical prediction [6] that a certain class of molecular Rydberg states formed by interaction of a Rydberg atom with a ground-state Rb atom can be stable at very large internuclear separation, comparable to the size of the Rydberg atoms. Even though the binding energies of these states are very small (of the order of 100 MHz), they are characterized by huge permanent dipole moments, which makes it possible to produce and manipulate these states by external fields in Bose-Einstein condensates.

Low-energy electron scattering by alkali-metal atoms has two distinctive features: a virtual ^3S state and a ^3P shape resonance [1,7,8]. The ^3P shape resonance occurs at very low energies (in meV energy range), and it is very hard to detect it experimentally [9]. An indirect information about the ^3P resonance can be obtained from experimental studies [10,11] of collisions of Rydberg atoms $A(nl)$ with ground-state atoms *B*. In particular the resonance increases substantially cross sections for inelastic transitions in $A(nl)$-*B* collisions and causes oscillatory behavior of the inelastic cross section as a function of the principal quantum number of the Rydberg state. These features allowed a prediction [1,2] of the ^3P resonance in *e*-Cs scattering whose existence was later confirmed by *ab initio* calculations [12] and a direct photodetachment experiment [13].

The ^3S and ^3P features in the electron scattering by alkali-metal atoms are crucial for formation of long-range molecular Rydberg states. They lead to oscillatory behavior of potential curves as functions of internuclear distances and local minima supporting localized vibrational states [6]. The ^3S-dominated states were dubbed "trilobite states" [6] due to specific shapes of their wave functions. The ^3P-dominated states also exhibit oscillations [14,15]. The oscillatory behavior of the potential curves can be well understood [16] in the framework of the Fermi pseudopotential approach [17]. The approach is valid when the interaction between the Rydberg electron and the neutral atom *B* can be described by a delta potential containing a single parameter, *e*-*B* scattering length. Several generalizations [18] of the Fermi approach introduce an energy-dependent scattering length. Another generalization proposed by Omont [19] introduces energy-dependent potential describing *P*-wave scattering. However, in the resonance region the pseudopotential is singular, and it is not clear how to avoid ambiguity in the treatment of this singularity. A more traditional approach to the potential curve calculation, based on the two-center expansion for the electron wave function, suffers from a poor convergence due to a very large number of coupled Rydberg states.

An alternative approach to the problem of a Rydberg electron interacting with a neutral atom was developed by Borodin and Kazansky [3]. It is based on solving the Lippman-Schwinger equation for the electron wave function containing the Coulomb Green's function of Hostler and Pratt [20] and modified by Davydkin *et al.* [21], to take into account the quantum defect of the Rydberg state. The Green's function incorporates the coupling of many degenerate Rydberg states leading to formation of so-called quasiadiabatic energy curves [3]. Assuming that the *e*-*B* interaction is dominated by the ^3P resonance and the electron's wave length is large compared to the effective radius of the *e*-*B* interaction, one can obtain a simple expression for the quasiadiabatic energy curves (atomic units are used throughout the paper) [2,3]

$$E_{1,2}=-1/[2(\nu_{1,2})]^2, \tag{1}$$

where $\nu_{1,2}$ are effective principal quantum numbers given by

$$\nu_1=n-\mu_0^f, \quad \nu_2=n-\delta(p(R))/\pi, \tag{2}$$

where μ_0^f is the fractional part of the quantum defect of the Rydberg state, $\delta(p)$ is the scattering phase shift in the ^3P symmetry, and $p(R)=(2/R-1/\nu^2)^{1/2}$ is the classical momentum of the electron in the Coulomb field of A^+.

The first solution in Eq. (2) gives a covalent Rydberg state whose energy, in the first approximation, is independent of the internuclear distance R, whereas the second solution results from the interaction between the ^3P resonance state and a degenerate manifold of Rydberg states. The interaction between these quasiadiabatic states leads to formation of adiabatic energy curves. Since the coupling between the quasiadiabatic states oscillates with n, this produces an oscillatory dependence of the inelastic collision cross section on n. In another case of scattering by an atom with a very low but positive electron affinity the coupling parameter depends on n exponentially, and this produces a sharp peak in the inelastic cross section [22].

The Borodin-Kazansky model [3], while providing a qualitative and semiquantitative understanding of the influence of the ^3P resonance on interaction between Rydberg atoms and ground-state alkali-metal atoms, contains several approximations which limit significantly the accuracy of the results. The most severe approximation is the assumption about the small radius of the e-B interaction which is not well justified because of high polarizabilities of alkali-metal atoms. Another drawback of previous calculations for alkali-metal containing Rydberg systems is that they do not include spin-orbit interaction that appears to be important in heavier alkali-metal atoms, Rb and Cs. The spin-orbit interaction leads to the fine-structure splitting of the ^3P resonance [12,23] of the order of few meV which is a substantial energy for this problem.

In the present paper, we extend the approach of Borodin and Kazansky by lifting the restriction on the radius of the e-B interaction. This can be accomplished by using the Kirchhoff-integral method [24] for matching the electron wave function in two regions of space: the region dominated by the e-B interaction and the region dominated by the e-A^+ interaction. The e-A^+ interaction can be taken into account exactly, using the Coulomb's Green function including the quantum defect [21]. Interaction of an electron with a neutral atom is presented by a pseudopotential, which reproduces correct phase shifts from the Dirac R-matrix calculations [23] and binding energies for corresponding negative ion. The obtained potential-energy curves can be employed for calculation of inelastic processes in A-B collisions and for calculations of properties of long-range molecular Rydberg states. One of their most important features are dipole moments that appear due to orientation of the Rydberg atom A in the presence of a perturber B. This problem is similar to orientation of a hydrogenlike atom in the presence of an external static field, and can be solved in a similar way. Specifically, we can construct the zero-order wave function for the system A-B using unperturbed Coulomb wave functions describing the e-A^+ interaction [25]. For the purpose of studying of a more general problem of collisions of Rydberg ions with neutrals, we discuss wave functions and dipole moments of atomic Rydberg states $A^{*,(Z-1)+}(n)$ perturbed by a neutral atom B. We apply results to the systems $\mathrm{Rb}^*(n=30)+\mathrm{Rb}(5s)$ and $\mathrm{Cs}^*(n=30)+\mathrm{Cs}(6s)$ [6]. This is important for understanding of how molecular Rydberg states interact with electromagnetic field, either by spontaneous emission or by coupling with a laser radiation. For example, the trilobite state discussed in Ref. [6] is dominated by the ^3S symmetry near the perturbing (ground-state Rb) atom. However, the state dominated by the ^3P symmetry is coupled by the dipole interaction with the ^3S-dominated state leading to the destruction of the latter.

The rest of the paper is organized as follows. In Sec. II we describe our method of potential curve calculations. Sec. III discusses a simplified approach based on the zero-range-potential model. Section IV discusses an analytical approach allowing us to obtain expressions for the wave functions outside the range of e-B interaction and dipole moments of the systems. Presentation of results given in Sec. V followed by Conclusion, Sec. VI.

II. SOLUTION OF THE ADIABATIC SCHRÖDINGER EQUATION BASED ON THE KIRCHHOFF-INTEGRAL APPROACH

A. Formulation

The Hamiltonian of the system $A(nl)+B(n_0s)$ reduces in the adiabatic approximation to the Hamiltonian of an electron in the presence of the neutral atom $B(n_0s)$ and the Coulomb center A^+. The corresponding Schrödinger equation is

$$\left(-\frac{1}{2}\nabla^2+\hat{V}(\vec{r})-\frac{1}{|\vec{r}-\vec{R}|}+V_{qd}(\vec{r}-\vec{R})-\frac{\alpha_d\vec{r}\cdot\vec{R}}{r^3R^3}-E^e_{M_J}(R)\right)\Psi_{M_J}(\vec{R},\vec{r})=0, \tag{3}$$

where $\hat{V}(\vec{r})$ is a nonlocal short-range potential for the e^--$B(n_0s)$ interaction, α_d is the polarizability of the atom B. Vector $\vec{R}$ is directed from the neutral center B to the Coulomb center A^+. V_{qd} is a short-range correction to the Coulomb potential which can be described by the quantum defect. We do not need the explicit form of V_{qd} if it is negligible outside the atomic core A^+. The coordinate system employed in this paper is presented in Fig. 1.

The fifth term in Eq. (3) describes three-body polarization interaction, that is e-B interaction due to polarization of B by A^+ plus A^+-B interaction due to polarization of B by e. Finally, the energy of the $B(n_0s)+A^+$ molecule is given by

$$E_{M_J}(R)=E^e_{M_J}(R)-\frac{\alpha_d}{2R^4},$$

where the last term describes the A^+-$B(n_0s)$ polarization interaction.

The pseudopotential for the e-B interaction is chosen in the form

$$\hat{V}(\vec{r})=\sum_\alpha g_{LS}(r)|\alpha\rangle\langle\alpha|, \tag{4}$$

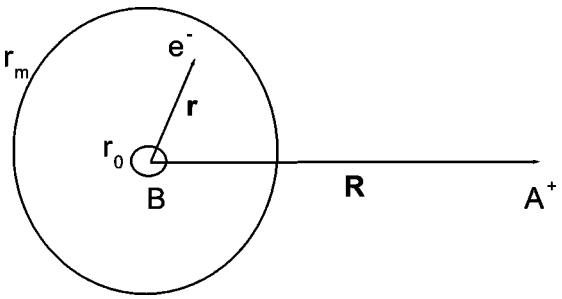

FIG. 1. Coordinate system employed in the paper. $\vec{R}$ is a vector directed from neutral atom B to the core A^+ of Rydberg atom. $\vec{r}$ is a vector pointed from neutral atom B to the valance electron. r_0 is the radius of the sphere within which we perform analytical Dirac calculation. r_m is the radius of the sphere outside which short-range interaction is negligible.

where

$$g_{LS}(r)=V_{LS}(r)+\frac{1}{2c^2r}\frac{dV_{LS}}{dr}(\vec{l}\cdot\vec{s}), \tag{5}$$

and $\vec{l}\cdot\vec{s}$ operator acts only on the Rydberg electron, since we assume that the valence electron is in the s state. α in Eq. (4) stands for $\{L,S,J\}$, quantum numbers of the orbital angular momentum, spin, and total angular momentum of two electrons relative to the neutral atom. $|\alpha\rangle$ is a two-electron spinor

$$\begin{aligned}|\alpha\rangle&=|LSJM_J\rangle\\&=\sum_{M_L,M_S}C^{JM_J}_{LM_LSM_S}|LM_L\rangle\sum_{\mu_1\mu_2}C^{SM_S}_{(1/2)\mu_1(1/2)\mu_2}\left|\frac{1}{2}\mu_1\right\rangle\\&\quad\times\left|\frac{1}{2}\mu_2\right\rangle,\end{aligned} \tag{6}$$

where $C^{JM_J}_{LM_LSM_S}$ are Clebsch-Gordon coefficients, $|LM_L\rangle$ are spherical harmonics, $|\frac{1}{2}\mu_1\rangle$, $|\frac{1}{2}\mu_2\rangle$ identify spin states of the Rydberg and the valence electrons, and M_J is the conserved projection of the total angular momentum on the quantization axis.

The nonlocal potential (4) describing e^--$B(n_0s)$ interaction has a local components (5) for certain angular momentum L and spin S of e^--$B(n_0s)$ system. Therefore, to find a solution to Eq. (3), we expand the wave function $\Psi_{M_J}(\vec{R},\vec{r})$ in two-electron spinors, Eq. (6)

$$\Psi_{M_J}(\vec{R},\vec{r})=\sum_{\alpha'}\frac{1}{r}u_{\alpha'}(r,R)|\alpha'\rangle. \tag{7}$$

After substituting Eq. (7) into Eq. (3), neglecting V_{qd}, and projecting on $\langle\alpha|$, we obtain the following system of differential equations

$$\begin{aligned}&\left(-\frac{1}{2}\frac{d^2}{dr^2}-\frac{L(L+1)}{2r^2}+V_{LS}(r)-E^e_{M_J}(R)\right)u_\alpha(r,R)\\&\quad=\sum_{\alpha'}\left(D_{\alpha\alpha'}(r,R)-\frac{1}{2c^2r}\frac{dV_{L'S'}}{dr}B_{\alpha\alpha'}\right)u_{\alpha'}(r,R),\end{aligned}$$

where

$$D_{\alpha\alpha'}(r,R)=\left\langle LSJM_J\left|\frac{1}{|\vec{r}-\vec{R}|}+\frac{\alpha_d\vec{r}\cdot\vec{R}}{r^3R^3}\right|L'S'J'M_J\right\rangle$$

and

$$B_{\alpha\alpha'}=\langle LSJM_J|\vec{l}\cdot\vec{s}|L'S'J'M_J\rangle.$$

Using Eq. (6) and the expansion

$$\frac{1}{|\vec{r}-\vec{R}|}=\sum_l\frac{r^l}{R^{l+1}}\sqrt{\frac{4\pi}{2l+1}}Y_{l0}(\hat{r})\quad(r<R) \tag{8}$$

and choosing z axis along $\vec{R}$, we obtain

$$\begin{aligned}D_{\alpha\alpha'}(r,R)&=\delta_{SS'}\frac{(-1)^{S-M_J}}{R}\\&\quad\times\sqrt{(2J+1)(2J'+1)(2L+1)(2L'+1)}\\&\quad\times\sum_{l=|L-L'|}^{L+L'}\left[\left(\frac{r}{R}\right)^l+\frac{\alpha_d}{r^2R}\delta_{l1}\right]\begin{pmatrix}L&l&L'\\0&0&0\end{pmatrix}\\&\quad\times\begin{pmatrix}J&l&J'\\M_J&0&-M_J\end{pmatrix}\begin{Bmatrix}L&L'&l\\J'&J&S\end{Bmatrix}.\end{aligned} \tag{9}$$

Symbols in parenthesis and braces denote $3j$ and $6j$ coefficients, respectively.

For $B_{\alpha\alpha'}$ we obtain

$$\begin{aligned}B_{\alpha\alpha'}&=(-1)^L\delta_{JJ'}\delta_{LL'}L(L+1)\\&\quad\times\sqrt{(2S+1)(2S'+1)}\sum_{j=L-(1/2)}^{L+(1/2)}(-1)^{j-L+(1/2)}\\&\quad\times\begin{Bmatrix}L&S&J\\\frac{1}{2}&j&\frac{1}{2}\end{Bmatrix}\begin{Bmatrix}L&S'&J\\\frac{1}{2}&j&\frac{1}{2}\end{Bmatrix}.\end{aligned}$$

The sum in Eq. (7) converges fast, and can be truncated at a relatively low L_{max}. In our calculation $L_{max}=2$ gives stable results. A general solution of the system of $4L_{max}+2$ second-order differential equations is a linear combination of $4L_{max}+2$ linear-independent solutions regular at the origin

$$u_\alpha(r,R)=\sum_{\alpha'}A_{\alpha'}v_{\alpha\alpha'}(r,R), \tag{10}$$

where α' enumerates independent solutions, and $A_{\alpha'}$ are constants.

TABLE I. Approximate mean values of quantum defects δ_l for $n>10$ [35,36].

L	0	1	2	3	4	5
Cs	4.05	3.60	2.50	0.03	0.011	0.002
Rb	3.13	2.65	1.34	0.02	0.004	0.001

To find the energy of the system and coefficients $A_{\alpha'}$, we use the Kirchhoff-integral method [24]. Green's function for the Coulomb field with quantum defect satisfies the following equation:

$$\left(-\frac{1}{2}\nabla^2-\frac{1}{|\vec{r}-\vec{R}|}+V_{qd}(\vec{r}-\vec{R})-E^e_{M_J}(R)\right)G(\vec{r}-\vec{R},\vec{r}'-\vec{R},E^e_{M_J}(R))=-\delta(\vec{r}-\vec{r}'), \tag{11}$$

where $G(\vec{r},\vec{r}',E)=G_0(\vec{r},\vec{r}',E)+G_{qd}(\vec{r},\vec{r}',E)$. $G_0(\vec{r},\vec{r}',E)$ is the Green's function for a pure Coulomb field and $G_{qd}(\vec{r},\vec{r}',E)$ is a correction due to the quantum defect. The Coulomb Green's function is [20]

$$G_0(\vec{r},\vec{r}',E)=-\frac{\Gamma(1-\nu)}{2\pi|\vec{r}-\vec{r}'|}[W_{\nu 1/2}(x)M'_{\nu 1/2}(y)-W'_{\nu 1/2}(x)M_{\nu 1/2}(y)], \tag{12}$$

where

$$x=\frac{1}{\nu}(r+r'+|\vec{r}-\vec{r}'|),$$

$$y=\frac{1}{\nu}(r+r'-|\vec{r}-\vec{r}'|)$$

and W and M are Whittaker's functions. The quantum defect correction has the following form [21]:

$$G_{qd}(\vec{r},\vec{r}',E)=\frac{\nu-1}{rr'}\sum_l\frac{\Gamma(1+l-\nu)\sin\,\pi(\mu_l+l)(2l+1)}{\Gamma(1+l+\nu)\sin\,\pi(\mu_l+\nu)4\pi}\times W_{\nu l+1/2}\left(\frac{2r}{\nu}\right)W_{\nu l+1/2}\left(\frac{2r'}{\nu}\right)P_l(\cos\gamma), \tag{13}$$

where μ_l are quantum defects given in Table I, γ is the angle between $\vec{r}$ and $\vec{r'}$ and $P_l(x)$ are Legendre polynomials.

We now multiply Eq. (3) by $G(\vec{r}-\vec{R},\vec{r}'-\vec{R},E^e_{M_J}(R))$, Eq. (11) by $\Psi_{M_J}(\vec{R},\vec{r})$, subtract one from another, and integrate over $\vec{r}$. Then we obtain

$$\oint_S\left(G(\vec{r}-\vec{R},\vec{r}'-\vec{R},E^e_{M_J}(R))\frac{d}{dr}\Psi_{M_J}(\vec{R},\vec{r})-\Psi_{M_J}(\vec{R},\vec{r})\frac{d}{dr}G(\vec{r}-\vec{R},\vec{r}'-\vec{R},E^e_{M_J}(R))\right)ds+\int_V\hat{V}(\vec{r})G(\vec{r}-\vec{R},\vec{r}'-\vec{R},E^e_{M_J}(R))\Psi_{M_J}(\vec{R},\vec{r})d\vec{r}=0, \tag{14}$$

where V is the volume outside the sphere of radius r_m around the neutral center B and S is the surface enclosing this volume. Here we use transformation of volume integral to the surface integral for the part which contains kinetic energy operator and take $r'\to r_m-0$ which gives zero contribution from the delta function.

The integrand in the volume integral contains the short-range potential $\hat{V}$. Therefore, if the radius of the sphere is big enough, its contribution is small. $\hat{V}$ outside the atom behaves like $\alpha_d/2r^4$. Therefore r_m can be determined from the condition $\alpha_d/2r_m^4\ll 1/(R+r_m)$. Thus only the surface integral contributes to the left-hand side. of Eq. (14). This gives us a matching condition for the wave function. In order to determine the energy, we have to substitute expansion for the wave function, Eqs. (7) and (10), into Eq. (14) and project on $\langle\alpha|$. We obtain

$$\sum_\alpha A_{\alpha''}M_{\alpha\alpha''}(E^e_{M_J})=0, \tag{15}$$

where

$$M_{\alpha\alpha''}(E^e_{M_J})=\sum_{\alpha'}\delta_{SS'}\sum_{M_LM_S}C^{JM_J}_{LM_LSM_S}C^{J'M_J}_{L'M_LSM_S}\times\left(\langle LM_L|G|L'M_L\rangle\frac{d}{dr}\frac{v_{\alpha'\alpha''}}{r}-\frac{v_{\alpha'\alpha''}}{r}\left\langle LM_L\left|\frac{dG}{dr}\right|L'M_L\right\rangle\right).$$

We have taken into account that Green's function depends only on difference of azimuthal angles $\varphi-\varphi'$ of $\vec{r}$ and $\vec{r}'$ vectors and therefore, $\langle LM_L|G|L'M'_L\rangle=\delta_{M_LM'_L}\langle LM_L|G|L'M_L\rangle$. Equation (15) is a homogeneous system of algebraic equations. It can have a nontrivial solution only if the determinant of $M_{\alpha\alpha'}(E^e_{M_J})$ is zero. This gives us an equation for determination of the energy. To determine A_α coefficients one additional condition is required, which is normalization. Some details of those calculation can be found in the Appendix.

B. Pseudopotentials for *e*-Rb and *e*-Cs interaction

There are basically two methods for the description of the effective interaction between an electron and a many-electron atom [26]: in the model-potential approach the effective interaction is attractive and leads to unphysical states

arising from the presence of filled atomic subshells. In this case, the scattering wave function contains the correct number of nodes, and the phase-shifts satisfy the generalized Levinson theorem [27]. In the alternative pseudopotential description the states corresponding to the inner-shell electrons are excluded by introducing a strong repulsive core [28]. For a treatment that should incorporate the spin-orbit interaction, the second method is not acceptable, because the spin-orbit interaction effects are most important at short distances, where the electron accelerates to high velocity due to the large nuclear charge. Therefore in the present paper, we use the model-potential method. However, we introduce a separate local potential for each scattering symmetry $|\alpha\rangle$. Thus the effective electron-atom interaction, Eq. (4), still can be called a pseudopotential.

For the S state of $B^-(n_0s)$ we adopted the following form for V_{LS} in Eq. (5) [29]

$$V_{0S}(r)=-\frac{A}{r}e^{-\gamma r}-\frac{\alpha}{2r^4}(1-e^{-(r/r_c)^6}), \tag{16}$$

while for the P-state we took

$$V_{1S}(r)=-\frac{Z_c}{r}e^{-\lambda r}-Ae^{-\gamma r}-\frac{\alpha}{2r^4}(1-e^{-(r/r_c)^6}). \tag{17}$$

The nuclear charge is Z_c, and λ is the nuclear screening parameter. Except for λ, all other parameters depend on L and S, and are determined from a fit reproducing the low-energy scattering eigenphases for $J\leqslant 2$ obtained from the Dirac R-matrix calculations [8,23] and binding energies of negative ions. We ignore the e-B interaction for $L>1$. In fitting procedure we take into account bound-states corresponding to complete subshells which are filled by inner electrons. Coefficients for the e-Cs potential were calculated by Bahrim *et al.* [29].

The spin-orbit interaction calculated according to Eq. (5) has an unphysical singularity $1/r^3$ at the origin. To fix this problem of the Pauli Hamiltonian we used the method introduced in Ref. [29]. In the region close to the origin, where the spin-orbit term diverges, we employ the big component $G_\kappa(r)$ of the Dirac wave function for the pure Coulomb field in the jj representation, and then transform it into the Pauli wave function at $r=r_0$ using the following equation:

$$U_{jl}(r)=\left[1-rf\frac{d^2}{dr^2}+\left(f-r\frac{df}{dr}\right)\frac{d}{dr}+\frac{\kappa(\kappa+2)}{r}-\kappa\frac{df}{dr}\right]G_\kappa(r), \tag{18}$$

where κ is the relativistic quantum number of the Dirac theory and $f(r)=\{8c^2[1-(V/2c^2)]^2\}^{-1}$. $G_\kappa(r)$ with a very good accuracy is given by the solution of the Dirac equation for the zero nonrelativistic energy

$$G_\kappa(r)=(\kappa-s)J_{2s}(y)+\frac{y}{2}J_{2s+1}(y),$$

TABLE II. The fit parameters for the pseudopotentials used to reproduce the scattering phase shifts by the Dirac R-matrix calculation [8]

	r_0	α	λ	state	A	γ	r_c
Rb	0.01	319.2	7.4975	^1S	4.5642	1.3438	1.8883
				^3S	68.576	9.9898	2.3813
				^1P	−4.2625	1.0055	1.8869
				^3P	−1.4523	4.8733	1.8160
Cs	0.01	402.2	7.2443	^1S	4.5396	1.3304	1.6848
				^3S	93.936	7.5397	2.6856
				^1P	−3.6681	1.3195	1.8031
				^3P	4.1271	2.2329	2.1294

where $s=\sqrt{\kappa^2-(Z_c^2/c^2)}$, $y=\sqrt{8Z_cr}$ and $J_s(y)$ is Bessel function. Finally, we transform the obtained function into the LS representation

$$u_{LSJ}=(-1)^{1+J-L}\sqrt{2S+1}\times\sum_{j=L-(1/2)}^{L+(1/2)}U_{jL}\sqrt{2j+1}\begin{Bmatrix}L & J & S\\ 1/2 & 1/2 & j\end{Bmatrix}. \tag{19}$$

All coefficients for the potentials are given in Table II and corresponding phase shifts for different states for Rb an Cs atoms are given in Figs. 2 and 3. In case $J=1$ we present the largest eigenphase of the two-channel problem. r_0 is chosen in such way that the nuclear screening is negligible at $r<r_0$, and at the same time the Coulomb electron-nuclear interaction is small compared to the electron rest energy at $r>r_0$. An order of magnitude estimate for r_0 is 0.01 a.u. In the ^3P case the relativistic effects (mainly, spin-orbit interaction) are important. Therefore, we start numerical integration with the function given by Eqs. (18) and (19). For the S states and for the singlet P state, we start with the nonrelativistic Coulomb wave function regular at the origin. To

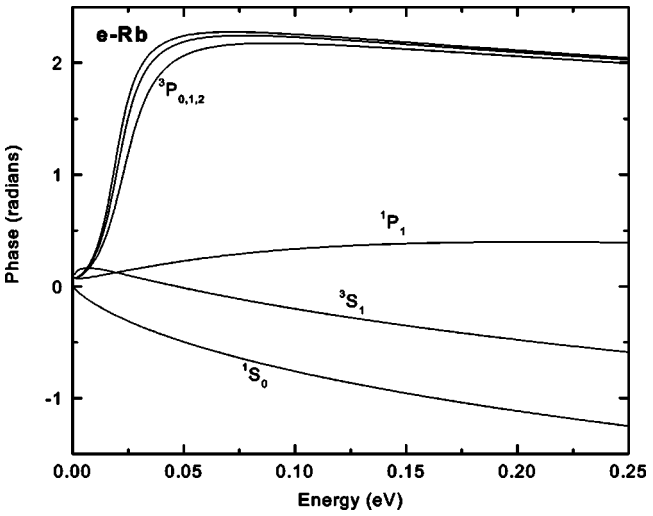

FIG. 2. Phase shifts for low-energy s- and p-wave electron scattering from Rb atom as a function of energy.

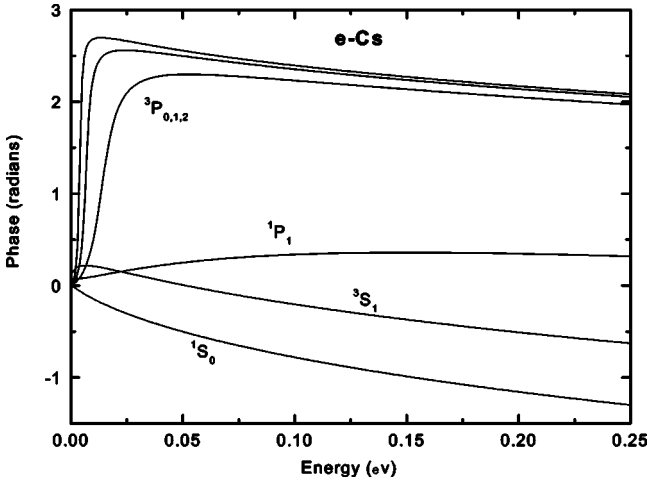

FIG. 3. Phase shifts for low-energy *s*- and *p*-wave electron scattering from Cs atom as a function of energy.

take into account a deviation from the pure Coulomb field, we expand potentials (16) and (17) at $r \to 0$, introduce effective charge Z_c^* and effective energy E^*, and write the regular function as

$$u_\alpha = M_{\nu^* l+(1/2)}(y),$$

where $\nu^* = Z_c^*/\sqrt{2E^*}$ and $y = \sqrt{8E^* r_0}$. For S states $Z_c^* = A$ and $E^* = A\gamma$, and for the singlet P-state $Z_c^* = Z_c$ and $E^* = Z_c\lambda - A$. $M_{\nu\mu}(r)$ is the Whittaker's function regular at the origin. As the initial condition for the states with L greater than 1, we take r_0^{L+1}.

III. ZERO-RANGE-POTENTIAL AND FERMI POTENTIAL WITH *P*-WAVE CONTRIBUTION

For comparison we also perform calculation in the zero-range-potential approximation [30] whereby e^--B interaction is modeled by a delta potential with the energy-dependent scattering parameter. Adiabatic energy levels of $A(nl)+B(n_0 s)$ system can be found by solving the equation [30]

$$\frac{-1}{A_s(k(R))} + 2\pi(G_{0r}(R,R,E(R)) + G_{qd}(R,R,E(R)) = 0, \tag{20}$$

where $A_s(k(R)) = -\tan\delta_s(k)/k$ is the effective triplet s-wave scattering length for electron collision with the ground-state $B(n_0 s)$ atom expressed through the scattering phase shift δ_s. $k(R)$ is defined as the classical momentum of the Rydberg electron

$$\frac{[k(R)]^2}{2} = \varepsilon + \frac{1}{R},$$

where ε is the Rydberg electron energy. Expression for G_{0r} in case of equal arguments has the following form:

$$G_{0r}(R,R,E) = \frac{Z\Gamma(1-\nu)}{\pi\nu}\left[\left(\frac{1}{4} - \frac{\nu}{x}\right) M_{\nu 1/2}(x) W_{\nu 1/2}(x) - M'_{\nu 1/2}(x) W'_{\nu 1/2}(x)\right],$$

where $x = 2ZR/\nu$. Equation (20) is the exact solution for the delta potential which takes into account only s wave. The correction due to p scattering can be incorporated using a generalization of the Fermi method proposed by Omont [19]. The energy of a state with a large quantum defect is given by

$$E_m(R) = E_{nl} + 2\pi A_s(k(R))|\Psi_{nlm}(\vec{R})|^2 + 6\pi A_p(k(R))|\nabla\Psi_{nlm}(\vec{R})|^2,$$

where $A_p = -\tan\delta_p/k^3$. In case of degenerate states, we have to diagonalize matrix $Q^m_{ll'}(R)$:

$$Q^m_{ll'}(R) = 2\pi A_s(k(R))\Psi^*_{nlm}(\vec{R})\Psi_{nl'm}(\vec{R}) + 6\pi A_p(k(R))\nabla\Psi^*_{nlm}(\vec{R})\nabla\Psi_{nl'm}(\vec{R}), \tag{21}$$

where $l = l_{min}, \ldots, (n-1)$ and $l' = l_{min}, \ldots, (n-1)$. l_{min} is the minimal angular momentum for which quantum defect is negligible.

To calculate gradients in Eq. (21), we use the formula [31]

$$\nabla\Psi_{nlm}(\vec{r}) = -\sqrt{\frac{l+1}{2l+1}}\left(\frac{dR_{nl}}{dr} - \frac{l}{r}R_{nl}\right)\vec{Y}^{l+1}_{lm}(\theta,\varphi) + \sqrt{\frac{l}{2l+1}}\left(\frac{dR_{nl}}{dr} + \frac{l+1}{r}R_{nl}\right)\vec{Y}^{l-1}_{lm}(\theta,\varphi),$$

where $\Psi_{nlm}(\vec{r}) = R_{nl}(r)Y_{lm}(\theta,\varphi)$ and $\vec{Y}^{l'}_{lm}(\theta,\varphi)$ are vector angular harmonics.

IV. WAVE FUNCTION AND DIPOLE MOMENT OF RYDBERG ELECTRON PERTURBED BY NEUTRAL ATOM

A. General equations for the wave function

In this section we use an analytical method to construct adiabatic wave functions of hydrogenlike Rydberg atom, perturbed by a neutral atom B. A free Rydberg atom can be described, for example, by Coulomb spherical wave functions $\psi_{nlm}(\vec{r})$. However, if this atom is perturbed by a neutral atom, the adiabatic Rydberg wave functions are significantly changed. Energy levels of excited states of hydrogenlike ions (H, He^+, Li^{++}, etc.) are degenerate, therefore outside the perturbing atom B the adiabatic Rydberg wave functions are significantly different from any single spherical function $\psi_{nlm}(\vec{r})$. These functions are equal to linear combinations of functions $\psi_{nlm}(\vec{r})$. For the solution of this problem we use the approach developed in Refs. [25,32].

We will neglect the quantum defect associated with the non-Coulomb part of the e-A^+ interaction and the spin-orbit interaction effects described in the previous section. On the other hand, we will add some generality by considering in-

teraction of Rydberg *ions* A^{Z-1} with the neutral atom *B*. Since the range of the *e*-*B* interaction is very small compared to the size of the Rydberg atom our analytical expressions for the wave functions turn out to be very close to numerical wave functions obtained from the Kirchhoff-integral method. However, the Kirchhoff-integral method is necessary for matching and obtaining adiabatic energy curves.

We start with the equation for the adiabatic wave function [25,32]

$$\Psi(\vec{R},\vec{r})=\int G(\vec{r},\vec{r}',E)\hat{V}(\vec{r})(|\vec{r}'-\vec{R}|)\Psi(\vec{R},\vec{r}')d\vec{r}'. \tag{22}$$

We will use the spectral representation of *G* which can be written as

$$G(\vec{r},\vec{r}\ ',E)=\sum_{nlm}\frac{\psi^*_{nlm}(\vec{r})\psi_{nlm}(\vec{r}')}{E-E_n}, \tag{23}$$

where the sum denotes summation over the discrete negative-energy states and integration over continuum.

If the wavelength of the Rydberg electron is large compared to the effective range of $\hat{V}(\vec{r})$ potential, we can expand the Green's function in powers of $(\vec{r}'-\vec{R})$

$$G(\vec{r}',\vec{r},E)\simeq G(\vec{R},\vec{r},E)+(\vec{r}'-\vec{R})\cdot\vec{\nabla}'G(\vec{r}',\vec{r},E)|_{\vec{r}'=\vec{R}}+\cdots, \tag{24}$$

and for the first nonvanishing term in expansion of $\Psi(\vec{R},\vec{r})$ we obtain

$$\Psi_{L=0}(\vec{R},\vec{r})=N_0G(E,\vec{r},\vec{R}),\quad L=0, \tag{25}$$

$$\Psi^{(k)}_{L=1}(\vec{R},\vec{r})=N_1\frac{\partial G}{\partial\{x_k\}}|_{\vec{r}'=\vec{R}},\quad L=1, \tag{26}$$

where $x_k, k=1,2,3$ are Cartesian coordinates of $\vec{r}$, x_3 axis is directed along $\vec{R}$ and $N_{0,1}$ are normalization factors. *L* is the orbital momentum corresponding to the symmetry of the electron wave function near the center *B*. As in the previous section, we concentrate on two cases, $L=0$ and $L=1$ relevant to the ^3S and ^3P *e*-*B* scattering.

Expansion (25) is valid if the electric field ($\simeq Z/R^2$) of the atomic Rydberg core does not perturb significantly the potential well of the atom *B*. For the system $Rb^*(n=30)+Rb(5s)$ this is valid at the internuclear distances $R\geqslant 100a_0$ whereas the size of Rydberg orbit with $n=30$ is $1800a_0$.

B. The case $L=0$

If the stable negative ion B^- exists, the Born-Oppenheimer potential curves of the system $A(nl)$-*B* can be separated into two classes: ionic and covalent curves. Each adiabatic curve of the system changes its character from ionic to covalent near the avoided crossing. The energy of the covalent state with negligible quantum defect is close to the energy of the hydrogenlike atom $E_n=-Z^2/2n^2$, therefore, the wave functions (25) are given mainly by the resonant term in the spectral representation of the Coulomb Green's function. For $L=0$ this function is, therefore, reduced to a sum of products of Coulomb wave functions $\psi_{nlm}(\vec{r})$ over the degenerate manifold, $\Psi_n(\vec{R},\vec{r})\cong\Sigma_{l,m}\psi^*_{nlm}(\vec{r})\psi_{nlm}(\vec{R})$. This sum has been expressed [25,32] through a quadratic form of only one wave function with zero angular momentum $l=m=0$. The wave function of the Rydberg electron for the $L=0$ dominated state and for an arbitrary principal quantum number *n* is [25,32]

$$\Psi_n(\vec{R},\vec{r})\equiv\frac{\sum_{l,m}\psi^*_{nlm}(\vec{r})\psi_{nlm}(\vec{R})}{\sqrt{Q_n(R)}}$$
$$=\left(\frac{4Z^2}{n^2}\right)\frac{\phi'_{n0}(y)\phi_{n0}(x)-\phi_{n0}(y)\phi'_{n0}(x)}{(x-y)\sqrt{Q_n(R)}}, \tag{27}$$

where the inverse square of the normalization constant is

$$Q_n(R)\equiv\sum_{l,m}|\psi_{nlm}(\vec{R})|^2=\left(\frac{d\phi_{n0}(R)}{dR}\right)^2+2\left(E_n+\frac{Z}{R}\right)\phi^2_{n0}(R), \tag{28}$$

and $x,y=(Z/n)(r+R\pm|\vec{r}-\vec{R}|)$, where $\phi_{n0}(x)=x\psi_{n0}(x)$ are wave functions for zero angular momentum $l=m=0$.

Using functions (27) we can rewrite the spectral representation (23) of the Coulomb Green's function in the following form

$$G(\vec{R},\vec{r},E)=\sum_n\frac{(Q_n(R))^{1/2}\Psi_n(\vec{R},\vec{r})}{E-E_n}, \tag{29}$$

where for every principal quantum number *n* only one wave function Ψ_n out of n^2 functions of the degenerate manifold is present.

C. The case $L=1$

In this case we have three possible covalent wave functions:

$$\Psi^{(k)}\simeq\frac{\partial G}{\partial x'_k}|_{\vec{r}'\to\vec{R}}, \tag{30}$$

where the derivatives of the Coulomb Green's function are

$$\left.\frac{\partial G}{\partial x'_k}\right|_{\vec{r}'\to\vec{R}}=\frac{(x_b)_k}{r_b}\frac{\Gamma(1-Z\nu)}{2\pi}\cdot\frac{F_k\{M,W\}}{|\vec{r}-\vec{R}|}, \tag{31}$$

where $\vec{r}_b\equiv\vec{r}-\vec{R}$. If x_3 axis is directed along vector $\vec{R}$, $F_k\{M,W\}$ are given by the equations

$$F_3\{M,W\}=\frac{2}{\nu}W'M'+\left(-\frac{1}{2\nu}+\frac{Z\nu}{R}\cdot\frac{R-r}{R-x_3}\right)WM$$
$$-\frac{WM'-W'M}{|\vec{R}-\vec{r}|}, \tag{32}$$

$$F_{1,2}\{M,W\}=\frac{2}{\nu}W'M'+\left(-\frac{1}{2\nu}+\frac{Z\nu}{R}\cdot\frac{r+R}{r+x_3}\right)WM - \frac{WM'-W'M}{|\vec{R}-\vec{r}|}. \quad (33)$$

$\Psi^{(3)}$ represents the state with zero projection of the orbital angular momentum L on the internuclear axis, $m=0$ (Σ state), whereas $\Psi^{(1,2)}$ represent the (real) states with $|m|=1$ (Π states).

After taking the limit $E\to E_n$ in Eqs. (31), (32), and (33) we obtain the wave function of the $L=1$ dominated state of Σ ($m=0$) symmetry [25]

$$\Psi_n^{(3)}(\vec{R},\vec{r}) \equiv\sum_{l,m}\frac{\psi^*_{nlm}(\vec{r})}{\sqrt{Q_n^{(3)}(R)}}\frac{d\psi_{nlm}(\vec{R})}{dR} =-\frac{4Z^2\cos\theta_b}{n^2|\vec{r}-\vec{R}|\sqrt{Q_n^{(3)}(R)}} \times\left[\frac{\phi'_{n0}(y)\phi_{n0}(x)-\phi_{n0}(y)\phi'_{n0}(x)}{y-x}+\phi'_{n0}(x)\phi'_{n0}(y) +\left(-\frac{1}{4}+\frac{n^2}{2ZR}\frac{R-r}{R-x_3}\right)\phi_{n0}(x)\phi_{n0}(y)\right], \quad (34)$$

where the inverse square of the normalization constant is

$$Q_n^{(3)}(R)=\sum_{lm}\left|\frac{d\psi_{nlm}(\vec{R})}{dR}\right|^2=\frac{2}{3}\left(E_n+\frac{Z}{R}\right)Q_n(R) + \frac{2Z}{3R^3}[\phi^2_{n0}(R)-2R\phi_{n0}(R)\phi'_{n0}(R)] \quad (35)$$

and for $|m|=1$

$$\Psi_n^{(1,2)}(\vec{R},\vec{r}) \equiv\sum_{l,m}\frac{\psi^*_{nlm}(\vec{r})}{\sqrt{Q_n^{(1,2)}(R)}}\frac{\partial\psi_{nlm}(\vec{R})}{\partial\{x_1,x_2\}}\bigg|_{\vec{r}'=\vec{R}} =-\frac{(x_b)_k}{r_b}\frac{4Z^2}{n^2|\vec{r}-\vec{R}|\sqrt{Q_n^{(1)}(R)}} \times\left[\frac{\phi'_{n0}(y)\phi_{n0}(x)-\phi_{n0}(y)\phi'_{n0}(x)}{y-x}+\phi'_{n0}(x)\phi'_{n0}(y) +\left(-\frac{1}{4}+\frac{n^2(r+R)}{2ZR(r+x_3)}\right)\phi_{n0}(x)\phi_{n0}(y)\right], \quad (36)$$

$$Q_n^{(1)}(R)=\frac{1}{R^2}\sum_{lm}\left|\frac{\partial\psi_{nlm}(\vec{R})}{\partial\theta}\right|^2_{\theta=0}=\frac{2}{3}\left(E_n+\frac{Z}{R}\right)Q_n(R) - \frac{Z}{3R^3}[\phi^2_{n0}(R)+R\phi_{n0}(R)\phi'_{n0}(R)]. \quad (37)$$

Functions $\Psi_n(\vec{R},\vec{r})$, Eq. (27), and $\Psi_n^{(k)}(\vec{R},\vec{r})$, Eqs. (34) and (36) are wave functions of atomic Rydberg states $A^{(Z-1)+}(n)$ perturbed by neutral atom B. They correspond to the reconstructed basis of degenerate states. These functions are correct outside the atom B and should be joined with the exact solution near the atom B as described in the previous section.

In Fermi approach [19] the potential energies of Rydberg electron interaction with atom B are equal to

$$E_{S\Sigma}(R)=2\pi A_s(k(R))|\Psi_n(\vec{R},\vec{r})|^2_{\vec{r}=\vec{R}}=2\pi A_s(k(R))Q_n(R), \quad (38)$$

$$E_{P\Sigma}(R)=6\pi A_p(k(R))\left|\frac{d\Psi_n^{(3)}(\vec{R},\vec{r})}{dr}\right|^2_{\vec{r}=\vec{R}} =6\pi A_p(k(R))Q_n^{(3)}(R). \quad (39)$$

D. Dipole moments

Since the constructed wave functions are linear combinations of states with different l, they generate a nonzero dipole moment $d_n(R)$:

$$d_n(R)=\langle\Psi_n|r\cos\theta|\Psi_n\rangle=\int r\cos\theta|\Psi_n(\vec{R},\vec{r})|^2d^3r, \quad (40)$$

where θ is the polar angle of the electron vector $\vec{r}$. It can be expressed through the radial matrix elements of r [33]:

$$r_{nl}\equiv\int rf_{nl-1}(r)f_{nl}r^2dr=-\frac{3n}{2Z}\sqrt{n^2-l^2}\quad(n\geqslant 1), \quad (41)$$

where $f_{nl}(r)$ are Coulomb radial wave functions. The dipole moment (40) depends on the polar angle θ_R of the vector $\vec{R}$. If x_3 axis is directed along vector $\vec{R}$, then $\theta_R=0$ and the dipole moment (40) is expressed thrugh the products of the associated Legendre functions $P_l^{|m|}(0)P_{l-1}^{|m|}(0)$ with the same quantum numbers m which are not equal to zero only for $|m|=0$. The dipole moments of the Σ states described by functions (27) and (34) are

$$d_n^{(0)}(R)=\sum_{l=0}^{n-1}r_{n,l}\frac{lf_{n,l}(R)f_{n,l-1}(R)}{2\pi Q_n(R)}, \quad (42)$$

$$d_n^{(3)}(R)=\sum_{l=0}^{n-1}r_{n,l}\frac{lf'_{n,l}(R)f'_{n,l-1}(R)}{2\pi Q_n^{(3)}(R)}, \quad (43)$$

where the upper index 0 stands for the Σ^3S state and 3 for the Σ^3P state. The dipole moments of the Π states described by function (36) are

$$d_n^{(1)}(R)=\sum_{l=0}^{n-1} r_{nl}\frac{l(l^2-1)f_{nl}(R)f_{n,l-1}(R)}{4\pi R^2 Q_n^{(1)}(R)}, \qquad (44)$$

Note that this dipole moment is zero for $n=2$ since there is the term containing $\psi_{2S}(r)$ in the linear combination (36) turns to zero in this case.

Nondiagonal matrix elements of the dipole moment for transitions between different Rydberg states are

$$d_n^{(0,3)}(R)=\sum_{l=0}^{n-1} r_{n,l}\frac{l[f_{n,l-1}(R)f_{n,l}(R)]'_R}{4\pi\sqrt{Q_n(R)Q_n^{(3)}(R)}}, \qquad (45)$$

$$d_n^{(0,1)}(R)=-\sum_{l=0}^{n-1} r_{n,l}\frac{lf_{n,l-1}(R)f_{n,l}(R)}{4\pi R\sqrt{Q_n(R)Q_n^{(1,2)}(R)}}, \qquad (46)$$

$$d_n^{(3,1)}(R)=\sum_{l=0}^{n-1} lr_{n,l}\frac{(l-1)f'_{n,l}(R)f_{n,l-1}(R)-(l+1)f_{n,l}(R)f'_{n,l-1}(R)}{8\pi R\sqrt{Q_n^{(3)}(R)Q_n^{(1,2)}(R)}}, \qquad (47)$$

where $d_n^{(3,1)}(R)\equiv\langle\Psi_n^{(3)}|x_1|\Psi_n^{(1)}\rangle=d_n^{(3,2)}(R)\equiv\langle\Psi_n^{(3)}|x_2|\Psi_n^{(1)}\rangle$.

For investigation of behavior of wave functions of active states and their dipole moments in the limit $R\to\infty$, we express the Cartesian coordinates x_1,x_2 through the elliptic coordinates ξ,η: $x_1=ZR(1+\xi)/n$, $x_2=ZR(1+\eta)/n$, where $\xi,\eta=(r\pm|\vec{R}-\vec{r}|)/R$, and we use the determination of the function ϕ_{n0}:

$$\phi_{n0}(\tau)=\sqrt{\frac{Z}{4\pi n}}\tau\exp\left(-\frac{\tau}{2}\right)F(-n+1,2,\tau).$$

At large R, near the Coulomb center, the elliptic coordinates are close to the parabolic coordinates $\mu=r+x_3$, $\nu=r-x_3$: $\xi\simeq 1-\nu/R+\cdots$, $\eta\simeq -1+\mu/R+\cdots$. Using the asymptotic limit for $Q_n(R)$,

$$Q_n(R)\to n\psi_{n0}^2(R)\simeq\frac{1}{(n!)^2}\frac{Z^3}{\pi n^2}\left(\frac{2ZR}{n}\right)^{2n-2}\times\exp\left(-\frac{2ZR}{n}\right), \quad R\to\infty \qquad (48)$$

we obtain for the $L=0$-dominated function $\Psi_n(\vec{R},\vec{r})$

$$\Psi_n(\vec{R},\vec{r})\simeq\frac{Z^{3/2}}{n^2\sqrt{\pi}}\exp\left(-\frac{Z(\mu+\nu)}{2n}\right){}_1F_1\left(-n+1;1;\frac{Z\mu}{n}\right), \quad R\to\infty. \qquad (49)$$

This function describes a Stark state with parabolic quantum numbers n, $m=0$, $n_1=n-1$, $n_2=0$ [34]. The limit of the dipole moment (42) of the state $\Psi_n(\vec{R},\vec{r})$ is given by the limits of the radial wave functions $f_{nl}(R)$ and $f_{nl-1}(R)$ and by the limit of $Q_n(R)$:

$$d_n(R)\simeq\frac{3n(n-1)}{2Z}, \quad R\to\infty. \qquad (50)$$

The dipole moments of Stark states are $d=3n(n_1-n_2)/2Z$ [34]. At $R\to\infty$ the state $\Psi_n(\vec{R},\vec{r})$ has the maximum dipole moment among states with a given principal quantum number n. In this limit the center of the electron charge is displaced to the side of the neutral atom B. The function $\Psi_n^{(3)}(\vec{R},\vec{r})$ also has the limit (49) and the dipole moment (42) at $R\to\infty$.

Stark states are eigenstates of hydrogenlike ions in a static electric field. In our case atomic Rydberg electron interacts with a neutral atom B, and there is no electric field. However, Stark states are formed in the system $A^*(n)+B$ at large internuclear distances R due to the special symmetry of the Coulomb potential leading to degeneracy of the energy levels. Consequently, wave functions of active states are equal to sums of products of the Coulomb functions over degenerate manifolds. Dipole moments of these Stark states, formed as limits of wave functions of active states, are parallel to the internuclear axis and directed from perturbed atom B to the nucleus of Rydberg atom $A^*(n)$.

In the limit $R\to\infty$ the wave function $\Psi_n^{(1,2)}(\vec{R},\vec{r})$, Eq. (25), is

$$\Psi_n^{(1,2)}(\vec{R},\vec{r})\to\psi_{n,|m|,n_1}(\mu,\nu,\phi)=Z^{5/2}\frac{\sqrt{2(n-1)}}{n^3}\sqrt{\mu\nu}\exp\left(-\frac{Z(\mu+\nu)}{2n}\right)\times F\left(-n+2;2;\frac{Z\mu}{n}\right)\frac{\{\cos\phi,\sin\phi\}}{\sqrt{\pi}}$$
$$(n,|m|=1,n_1=n-2), \quad R\to\infty. \qquad (51)$$

This Stark state has the maximum dipole moment for $|m|=1$, $d_{n,|m|=1}^{max}=3n(n-2)/2Z$.

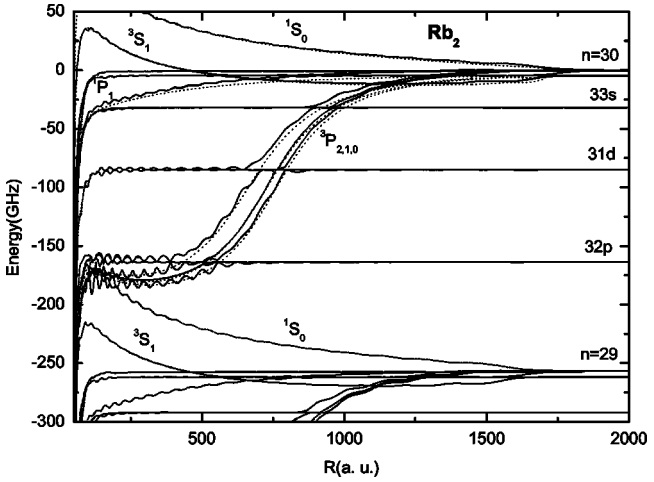

FIG. 4. Born-Oppenheimer potential curves for Rb_2 Rydberg molecule. Full lines: calculation with Kirchhoff-integral approach; Dashed lines: quasiclassical calculations with Borodin-Kazansky model. The zero of the energy axis is taken to lie at the position of the $n=30$ manifold with projection of total momentum $M_J=0$.

V. RESULTS AND DISCUSSION

In Figs. 4–7 we present results of our calculations of the energy curves of Rb_2 and Cs_2 molecular Rydberg states with projection of total angular moment $M_J=0$. The curves are shown for the energy range lying between $n=29$ and $n=30$. Each level is marked by the dominant symmetry near the perturber *B*.

From each hydrogenic state we have six split levels, which correspond to the $^1S_0$, $^1P_1$, $^3S_1$, $^3P_0$, $^3P_1$, and $^3P_2$ symmetry of valence electron relative to the neutral atom. In addition to that, the levels are marked by quantum numbers of Rydberg atom *A* corresponding to energy levels of separated atoms. There are two distinctive features caused by the presence of the ^3P-dominated states. First, the *P*-wave contribution significantly modifies energy spectra. Second, interaction of the split *P* levels with other pseudocrossed levels causes enhancement of oscillations.

Spin-orbit interaction leads to the splitting of the ^3P energy levels. This splitting is especially crucial for the Cs_2 molecule (cf. Fig. 5), where the ^3P resonance occurs at very low energy which corresponds to $R\approx 1000$ a.u. for $n=30$.

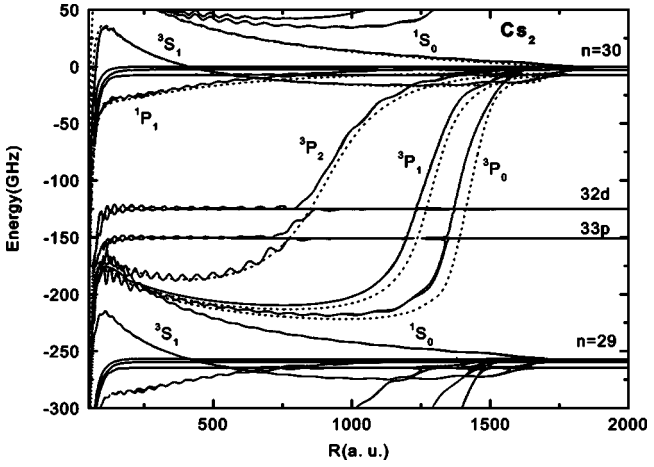

FIG. 5. The same as in Fig. 4 for Cs_2 molecule.

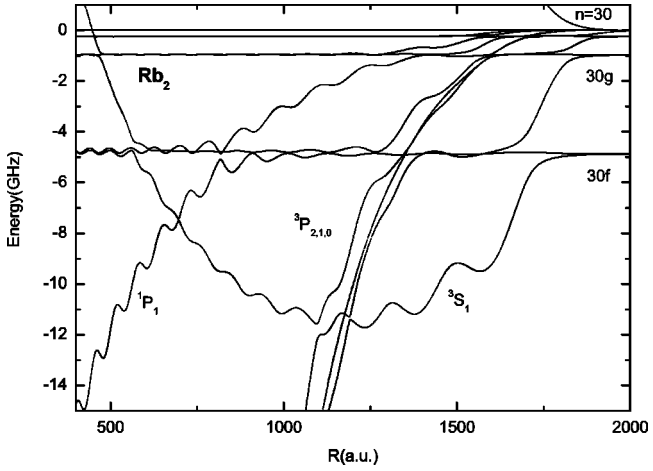

FIG. 6. The same as in Fig. 4. The region close to $n=30$ is enlarged.

Note that only the curves corresponding to $J=0,2$ symmetry oscillate as functions of internuclear distance. Indeed, due to properties of Clebsch-Gordan coefficients only the $M_L=\pm 1$ states contribute to the wave function of the $J=1$ state, therefore the latter is in fact a Π state. The corresponding wave function is oriented perpendicular to the internuclear axes. In this direction behavior of radial part is monotonic, and energy curves also behave monotonically. In contrast the wave functions of the $^3P_{0,2}$ states contain the Σ component which reflects the oscillatory behavior of the radial wave function along the internuclear axis. These oscillations lead to the oscillatory behavior of the adiabatic energy curves. Recent calculations for Rb_2 [15] based on a generalization of the Fermi approach also confirm that the Π curve does not oscillate

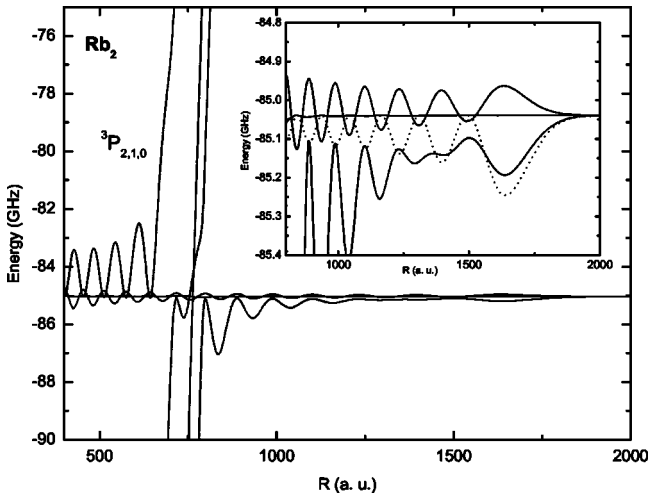

FIG. 7. The Born-Oppenheimer potential curve for the low-*l* class of Rydberg states of the Rb_2 molecule formed from $31d+5s$ states of separated atoms. Full line: Kirchhoff-integral approach where $M_J=0$; dotted line: ZPR model calculation with $M_L=0$.

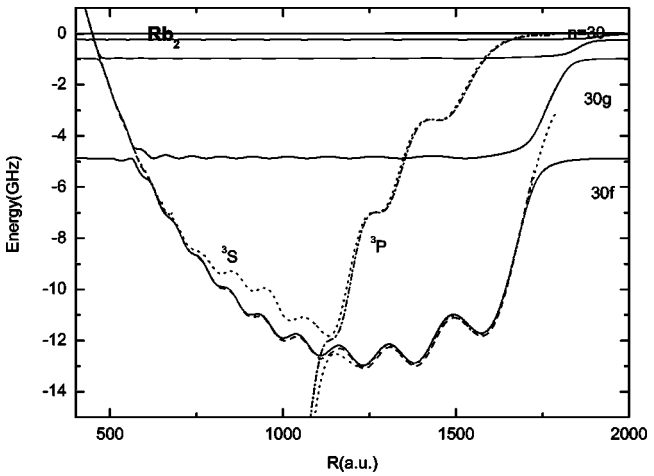

FIG. 8. $Rb_2\Sigma$ states. Full lines: calculation with the zero-range potential model; dotted lines: the Fermi model with the *p*-wave contribution; dashed line: $E_{S_\Sigma}(R)$ using formula (38); dash-dotted line: $E_{P_\Sigma}(R)$ using formula (39).

In Fig. 6 we present the same energy curves for Rb_2 with enlarged region close to the level $n=30$ where the curves behavior becomes complicated due to the spin-orbit splitting and multiple pseudocrossings. The deepest minimum in the ^3S-dominated curve is destroyed by a pseudocrossing with the $^3P_{0,1,2}$ curves, but local minima still exist with the potential barrier whose width is about 100 a.u.

In Fig. 7 we present energy curves corresponding to states which originate from the $31d+5s$ state of separated atoms. The dotted line represents the result obtained using ZPR model with the energy-dependent scattering length. The energy curves in the nested graph do not correspond to any particular symmetry relative to the ground-state atom. For $M_J=0$ all curves are superposition of Σ and Π states. More oscillatory energy curves are dominated by Σ symmetry. The energy curves are significantly modified due to interaction with the ^3P levels, but one important minimum at distance $R\approx 1600$ a.u., which supports several vibrational states [6], still exists.

Behavior of the *S*-dominated curves can be understood in terms of the ZPR or the Fermi model with energy-dependent scattering length [6]. They reproduce energy curves close to exact calculation in the regions where there is no contribution from the *P*-dominated levels. The *P* levels, on the other hand, can be obtained employing the method developed by Omont [19], which is a generalization of the Fermi potential model. Corresponding energy levels are shown in Fig. 8. The region close to $R\approx 700$ a.u. is dominated by the *P* resonance in *e*-Rb scattering (Fig. 2), and here the Omont's formula is no longer valid, since it contains a divergent effective scattering length. Analytical results obtained in the previous section [formula (38) and (39)] for the potentials $E_{S\Sigma}(R)$ and $E_{P\Sigma}(R)$ are also shown in Fig. 8. Overall behavior of energy levels can be well described by the Borodin and Kazansky model [3]

$$E(R)=-\frac{1}{2\left(n-\frac{\delta(p(R))}{\pi}\right)^2}-\frac{\alpha_d}{2R^4}, \qquad (52)$$

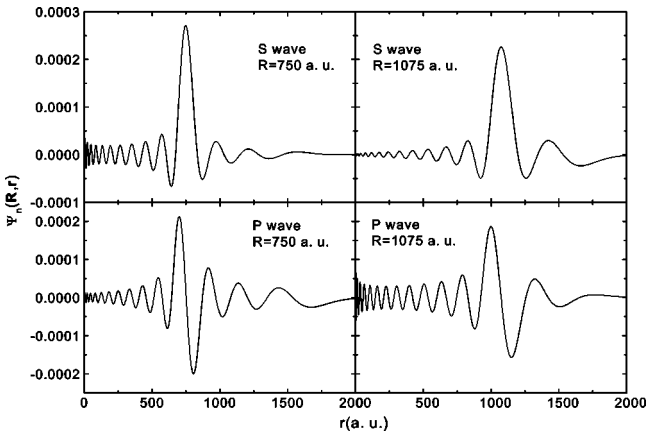

FIG. 9. The wave functions $\Psi_n(\vec{R},\vec{r})$ for *S*- and *P*-dominated states, Eqs. (27) and (34), plotted versus distance *r* of Rydberg electron from A^+ along the internuclear axis $\vec{R}$, for internuclear distances $R=750$ a.u. and $R=1075$ a.u. for Rb_2.

where $\delta(p(R))$ is the scattering phase shift and $p(R)=\sqrt{(2/R)-(1/\nu^2)}$. The energy curves are roughly determined by corresponding phase shifts for electron-neutral atom scattering, although the oscillations necessary for existence of stable molecular states cannot be described by simple Eq. (52). Behavior of the potential curves at relatively small internuclear distance is dominated by the polarization attraction between A^+ and *B*. This means that the global minimum can exist only at very small distances where potential curves turn up due to the repulsion between A^+ and *B*. (This region is not described by our model).

In Fig. 9 we present the electron wave functions $\Psi_n(\vec{R},\vec{r})$, Eqs. (27) and (34), calculated for internuclear distance $R=750$ a.u. and $R=1075$ and corresponding to the *S*- and *P*-dominated symmetries. The electron probability density is mostly concentrated near the neutral atom *B*. The comparison of the analytical wave function $\Psi_n(\vec{R},\vec{r})$, Eq. (27), with numerical results from the Kirchhoff-integral method for the internuclear distance $R=1230$ a.u. are presented in Fig. 10. Oscillatory behavior of the numerical wave function near the neutral atom *B* is due to the complex structure of the pseudopotential, which supports energy levels corresponding to the closed subshells of the neutral atom. The analytical wave function describes very well the actual wave function in the region outside atom *B*.

Dipole moments (42)–(47) are shown in Fig. 11. For $Z=1$ and $n=30$ the limiting value of dipole moments (42) and (43) is 1305 a.u. and the limiting value of the dipole moment (44) is 1260 a.u. Nondiagonal matrix elements shown in Fig. 11(b) have different dependence on *R* and in the region of classically allowed motion of Rydberg electron they are smaller than the diagonal matrix element.

VI. CONCLUSION

We have calculated adiabatic energy curves for diatomic Rydberg Cs_2 and Rb_2 molecules. Our results confirm qualitatively and semiquantitavely previous data obtained by

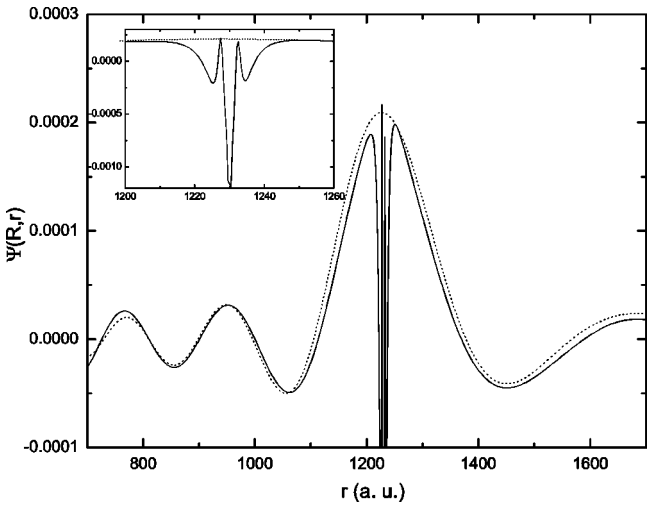

FIG. 10. The comparison of the wave function $\Psi_n(\vec{R},\vec{r})$, Eq. (27), with the results of numerical calculations; internuclear distance $R=1230$ a.u. Full line corresponds to numerical result without spin-orbit interaction and with $M_L=0$ for Rb_2.

Greene *et al.* [6] for the ^3S-dominated (trilobite) states and predict a new class of ^3P-dominated states. Inclusion of spin-orbit interaction modifies considerably energy levels. Spin-orbit coupling is especially significant for the ^3P-dominated states in the Cs_2 molecule. At small distances adiabatic energy curves are dominated by polarization interaction between the ground-state atom and the Rydberg core which excludes possibility of existence of a global minimum in the energy curve at large internuclear distances. This means that all equilibrium configurations supported by local minima are in fact metastable states whose lifetime is determined by the probability of tunneling into adjacent potential wells.

The behavior of obtained energy curves is directly related to the electron-atom scattering phase shifts, which is well seen from comparison of our calculations with the Borodin and Kazansky model [3]. At the same time our results are more accurate than those obtained within the framework of the Borodin-Kazansky model since the latter assumes the small radius of the effective electron–atom interaction and ignores the spin-orbit interaction.

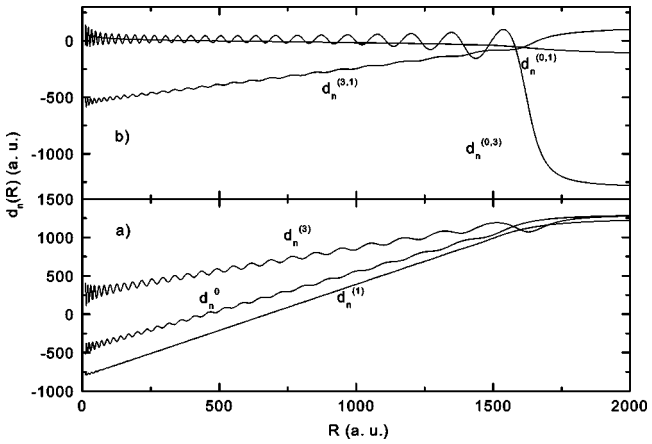

FIG. 11. (a) Dipole moments (42)–(44) of Rydberg electron in states with wave functions (27), (34), and (36) ($n=30$) as functions of internuclear distance R for Rb_2. (b) Nondiagonal dipole matrix elements (45)–(47) of Rydberg electron in states with wave functions (27), (34), and (36) ($n=30$) as functions of the internuclear distance R.

The obtained results can be applied to designing Rydberg molecules with huge dipole moment in the ultracold gas conditions in Bose-Einstein condensates. The dipole moment of the Rydberg states and transition dipole moments, calculated in the present paper, would help to explore how the long-range Rydberg states can be manipulated by laser radiation and external static fields and to calculate their lifetimes with respect to the spontaneous emission. On the other hand, studies of nonradiative nonadiabatic transitions between these states would allow an accurate treatment of collisions of Rydberg atoms with ground-state alkali-metal atoms.

ACKNOWLEDGMENTS

M.I.C. would like to thank the members of the atomic physics group for their hospitality during his visit to the University of Nebraska–Lincoln. This work was supported by NSF Grant No. PHY-0098459.

APPENDIX: MATRIX ELEMENTS OF THE GREEN'S FUNCTION

Green's function G_0 has singularity at $\vec{r}=\vec{r}'$. In order to avoid problems with numerical integration, we extract the diverging part $1/2\pi|\vec{r}-\vec{r}'|$ as

$$G_0(\vec{r}-\vec{R},\vec{r}'-\vec{R},E^e_{M_J})=G_{0r}(\vec{r}-\vec{R},\vec{r}'-\vec{R},E^e_{M_J})-\frac{1}{2\pi|\vec{r}-\vec{r}'|},$$

where G_{0r} is a regular part of the Green's function. The integrals of the singular part and its derivative are

$$\left\langle LM_L\left|\frac{1}{2\pi|\vec{r}-\vec{r}'|}\right|L'M_L\right\rangle=\frac{2\delta'_{LL}}{r_0(2L+1)}$$

and

$$-\left\langle LM_L\left|\frac{d}{dr}\frac{1}{2\pi|\vec{r}-\vec{r}'|}\right|L'M_L\right\rangle=\frac{2\delta'_{LL}(L+1)}{r_0^2(2L+1)}.$$

Matrix elements of the regular Green's function contain four-dimensional integration. Using cylindrical symmetry of the problem, they can be reduced to three-dimensional integrals.

In the G_{qd} correction to the Green's function Eq. (13), arguments of the Whittaker's functions, r and r', are independent of φ. Therefore, integration over φ can be performed analytically. For the matrix element of G_{qd} we have the following expression:

$$\langle LM_L|G_{qd}|L'M_L\rangle = -\sqrt{\frac{(2L+1)(2L'+1)(L-|M_L|)!(L'-|M_L|)!}{(L+|M_L|)!(L'+|M_L|)!}}\,\nu \sum_l \frac{\Gamma(1+l-\nu)\sin\pi(\mu+l)(2l+1)}{\Gamma(1+l+\nu)\sin\pi(\mu_l-\nu)4}$$

$$\times \int_{-1}^{1}\int_{-1}^{1} \frac{W_{\nu l+1/2}\left(\frac{2Zr(x)}{\nu}\right) W_{\nu l+1/2}\left(\frac{2Zr'(x')}{\nu}\right)}{r(x)r'(x')} F_{lM_L}(x,x') P_L^{|M_L|}(x) P_{L'}^{|M_L|}(x')\,dx\,dx'$$

and for its derivative

$$\left\langle LM_L\left|\frac{dG_{qd}}{dr}\right|L'M_L\right\rangle = -\sqrt{\frac{(2L+1)(2L'+1)(L-|M_L|)!(L'-|M_L|)!}{(L+|M_L|)!(L'+|M_L|)!}}\,\nu \sum_l \frac{\Gamma(1+l-\nu)\sin\pi(\mu+l)(2l+1)}{\Gamma(1+l+\nu)\sin\pi(\mu_l-\nu)4}$$

$$\times \int_{-1}^{1}\int_{-1}^{1} \left\{ \frac{W_{\nu l+1/2}\left(\frac{2r(x)}{\nu}\right) W_{\nu l+1/2}\left(\frac{2r(x')}{\nu}\right)}{r(x)r(x')} \left[\frac{Rx-r_0}{r(x)^2} F_{lM_L}(x,x') + K(x,x') G_{lM_L}(x,x') \right.\right.$$

$$\left.\left. + N(x,x') H_{lM_L}(x,x') \right] - \frac{W'_{\nu l+1/2}\left(\frac{2r(x)}{\nu}\right) W_{\nu l+1/2}\left(\frac{2r(x')}{\nu}\right)}{r(x)r(x')} \frac{2(Rx'-r)}{\nu r(x)} F_{lM_L}(x,x') \right\} dx\,dx',$$

where

$$F_{lM_L}(x,x') = \frac{1}{2\pi}\int_0^{2\pi} P_l(\cos\gamma) e^{iM_L\varphi} d\varphi$$

$$= \sum_{n=0}^{[L/2]} \sum_{k=M_L, k-M_L=even}^{L-2n} \frac{(-1)^n(2L-2n)!}{n!2^{k+L}(L-n)!(L-2n-k)!\left(\frac{k-M_L}{2}\right)!\left(\frac{k+M_L}{2}\right)!} b(x,x')^k a(x,x')^{L-2n-k},$$

$$G_{lM_L}(x,x') = \frac{1}{2\pi}\int_0^{2\pi} P_l'(\cos\gamma) e^{iM_L\varphi} d\varphi$$

$$= \sum_{n=0}^{[L/2]} \sum_{k=M_L k-M_L=even}^{L-2n-1} \frac{(-1)^n(2L-2n)!}{n!2^{k+L}(L-n)!(L-2n-1-k)!\left(\frac{k-M_L}{2}\right)!\left(\frac{k+M_L}{2}\right)!} b(x,x')^k a(x,x')^{L-2n-1-k},$$

$$H_{lM_L}(x,x') = \frac{1}{2\pi}\int_0^{2\pi} P_l'(\cos\gamma)\cos\varphi\, e^{iM_L\varphi} d\varphi$$

$$= \sum_{n=0}^{[L/2]} \sum_{k=\max(0,M_L-1), k-M_L-1=even}^{L-2n-1} \frac{(-1)^n(2L-2n)!(k+1)}{n!2^{k+L+1}(L-n)!(L-2n-1-k)!\left(\frac{k-M_L+1}{2}\right)!\left(\frac{k+M_L+1}{2}\right)!}$$

$$\times [b(x,x')]^k [a(x,x')]^{L-2n-1-k},$$

where

$$\cos\gamma = a(x,x') + b(x,x')\cos\varphi,$$

$$a = \frac{1}{2r(x)r(x')}[r(x)^2 + r(x')^2 - 2r_0 + 2r_0 xx'],$$

$$b = \frac{r_0}{r(x)r(x')}\sqrt{(1-x^2)(1-x'^2)},$$

$$r(x) = \sqrt{R^2 + r_0^2 - 2Rr_0 x},$$

$$K_{lM_L}(x,x') = \frac{r_0 xx' - Rx}{r(x)r(x')} + \frac{Rx - r_0}{r(x)^2}\,\frac{R^2 - r_0 Rx - r_0 Rx' + r_0^2 xx'}{r(x)r(x')},$$

$$N_{lM_L}(x,x') = \left(\frac{r_0}{r(x)r(x')} + \frac{Rx - r_0}{r(x)^2}\,\frac{r_0^2}{r(x)r(x')}\right) \times \sqrt{(1-x^2)(1-x'^2)}.$$

Green's function has poles at energies coinciding with undisturbed hydrogen levels. To avoid problem in numerical search for zeros, it is useful to multiply all matrix elements by the factor

$$\frac{\sum_l \sin\pi(\mu_l - \nu)}{\Gamma(1-\nu)},$$

which eliminates all energy poles in the matrix elements.

[1] I.I. Fabrikant, J. Phys. B **19**, 1527 (1986).
[2] V.M. Borodin, I.I. Fabrikant, and A.K. Kazansky, Phys. Rev. A **44**, 5725 (1991).
[3] V.M. Borodin and A.K. Kazansky, J. Phys. B **25**, 971 (1992).
[4] M. Chibisov *et al.*, J. Phys. B **30**, 991 (1997); M.I. Chibisov *et al.*, *ibid.* **31**, 2795 (1998); I.I. Fabrikant, *ibid.* **31**, 2921 (1998); I.I. Fabrikant and M.I. Chibisov, Phys. Rev. A **61**, 022718 (2000).
[5] V.P. Zhdanov and M.I. Chibisov, Zh. Éksp. Teor. Fiz. **74**, 75 (1978) [Sov. Phys. JETP **47**, 38 (1978)]; V.P. Zhdanov, J. Physiol. Biochem. **13**, L311 (1980); I.F. Schneider, A.E. Orel, and A. Suzor-Weiner, Phys. Rev. Lett. **85**, 3785 (2000); I.F. Schneider, O. Dulieu, and A. Giusti-Suzor, J. Phys. B **24**, L289 (1991); S.L. Guberman, Phys. Rev. A **49**, R4277 (1994).
[6] C.H. Greene, A.S. Dickinson, H.R. Sadeghpour, Phys. Rev. Lett. **85**, 2458 (2000); B.E. Granger, E.L. Hamilton, and C.H. Greene, Phys. Rev. A **64**, 042508 (2001).
[7] I.I. Fabrikant, Phys. Rev. A **45**, 6404 (1992); Comments At. Mol. Phys. **32**, 267 (1996).
[8] C. Bahrim, U. Thumm, and I.I. Fabrikant, J. Phys. B **34**, L195 (2001).
[9] A.R. Johnson and P.D. Burrow, J. Phys. B **15**, L745 (1982).
[10] H. Heinke, J. Lawrentz, K. Niemax, and K.-H. Weber, Z. Phys. A **312**, 329 (1983); K.-H. Weber and K. Niemax, Opt. Commun. **28**, 317 (1979).
[11] B.P. Stoicheff and E. Weinberger, Phys. Rev. Lett. **44**, 733 (1980); D.C. Thompson, E. Weinberger, G.-X. Xu, and B.P. Stoicheff, Phys. Rev. A **35**, 640 (1987).
[12] U. Thumm and D.W. Norcross, Phys. Rev. Lett. **67**, 3495 (1991); Phys. Rev. A **45**, 6349 (1992).
[13] M. Scheer *et al.*, Phys. Rev. Lett. **80**, 684 (1998).
[14] M.I. Chibisov, A.A. Khuskivadze, and I.I. Fabrikant, J. Phys. B **35**, L193 (2002).
[15] E.L. Hamilton, C.H. Greene, and H.R. Sadeghpour, J. Phys. B **35**, L199 (2002).
[16] N.Y. Du and C.H. Greene, Phys. Rev. A **36**, 471 (1987); **36**, 5467(E) (1987).
[17] E. Fermi, Nuovo Cimento **11**, 157 (1934); see, also, M. Matsuzava in *Rydberg States of Atoms and Molecules*, edited by R.F. Stebbings and F. B. Dunning (Cambridge University Press, Cambridge, 1983), p. 267.
[18] A.P. Hickman, Phys. Rev. A **23**, 87 (1981); E. de Prunele and J. Pascale, J. Phys. B **12**, 2511 (1979); V.S. Lebedev and I.I. Fabrikant, Phys. Rev. A **54**, 2888 (1996).
[19] A. Omont, J. Phys. (Paris) **38**, 1343 (1977).
[20] L. Hostler and R.H. Pratt, Phys. Rev. Lett. **10**, 469 (1963).
[21] V.A. Davydkin, B.A. Zon, N.L. Manakov, and L.P. Rapoport, Zh. Éksp. Teor. Fiz. **60**, 124 (1971) [Sov. Phys. JETP **33**, 70 (1971)].
[22] I.I. Fabrikant and V.S. Lebedev, J. Phys. B **33**, 1521 (2000).
[23] C. Bahrim and U. Thumm, Phys. Rev. A **61**, 022722 (2000); C. Bahrim, U. Thumm, and I.I. Fabrikant, *ibid.* **63**, 042710 (2001).
[24] I.I. Fabrikant, J. Phys. B **26**, 2533 (1993); D. B. Khrebtukov, Ph. D. thesis, University of Nebraska–Lincoln, 1995.
[25] M.I. Chibisov, Zh. Éksp. Teor. Fiz. **120**, 291 (2001) [JETP **93**, 256 (2001)].
[26] G. Peach, J. Phys. B **11**, 2107 (1978); P. Valiron, R. Gayet, R. McCarroll, F. Masnou-Seeuws, and M. Philippe, *ibid.* **12**, 53 (1979).
[27] P. Swan, Proc. R. Soc. London, Ser. A **228**, 10 (1955).
[28] J.N. Bardsley, Case Stud. At. Phys. **4**, 299 (1974).
[29] C. Bahrim, I.I. Fabrikant, and U. Thumm, Phys. Rev. Lett. **87**, 123003 (2001); **88**, 109904(E) (2002).
[30] Yu. N. Demkov and V.N. Ostrovskii, *Zero-Range Potentials and Their Applications in Atomic Physics* (Plenum Press, New York, 1988).
[31] D.A. Varshalovich, A.N. Moskalev, and V.K. Khersonskii, *Quantum Theory of Angular Momentum* (World Scientific, New Jersey, 1988).
[32] M.I. Chibisov, A.M. Ermolaev, F. Brouillard, and M.H. Cherkani, Phys. Rev. Lett. **84**, 451 (2000); M.I. Chibisov, A.M. Ermolaev, M. Cherkani, and F. Brouillard, Zh. Éksp. Teor. Fiz.

117, 313 (2000) [JETP **90**, 276 (2000)]; M.H. Cherkani, F. Brouillard, and M.I. Chibisov, J. Phys. B **34**, 49 (2001).
[33] V.B. Berestetskii, E.M. Lifshitz, and L.P. Pitaevskii, *Relativistic Quantum Theory* (Pergamon, Oxford, 1971), Vol. 1.
[34] L.D. Landau and E.M. Lifshitz, *Quantum Mechanics, Non-Relativistic Theory* (Pergamon, Oxford, 1965).
[35] H.G. Kuhn, *Atomic Spectra* (Longmans, Green, New York, 1964).
[36] C.E. Moore, Atomic Energy Levels (Natl. Bur. of Standards, Washington, DC, 1971).